Vortex Whistle in Radial Intake

Dr. Man-Chun Tse
Pratt & Whitney Canada Corp.
1000 Marie-Victorin, Longueuil, Quebec, Canada, J4G 1A1

E-mail : Man-Chun.Tse@pwc.ca

ABSTRACT

In a radial-to-axial intake with inlet guide vanes (IGV) at the entry, a strong flow circulation Γ can be generated from the tangential flow components created by the IGVs when their setting exceed about half-closing (≈45°). The circulation is convected downstream in the gaspath. As the flow area of the gaspath is reduced towards the axial-exit, the initial circulation is stretched. This increases the vorticity intensity as a result of conservation of circulation, leading to a strong audible vortex whistle tone, together with flow energy separation with up to 20°F difference between the hub and the shroud surfaces. A solution of suppressing the vortex whistle was found experimentally. This was achieved by installing 5 fences equally distributed at mid gaspath around the hub surface. Test results indicate that the vortex whistle (100-700Hz) can be suppressed by the fences, but at the expense of generating higher broadband noise at higher frequencies. Experimental results demonstrate that the vortex whistle fundamental frequency (fo) is equal to the swirling flow frequency (fs) evaluated at the viscous core of a Rankine-vortex model for the tangential flow velocity. It is concluded that a vortex whistle can generally be suppressed by preventing the buildup of vorticity intensity.

1.0 Introduction

A large aviation auxiliary power unit (APU) generally includes two compressors, namely the load and core compressors. This arrangement is intended to maximize the power output efficiency. The load compressor generally runs at constant rpm, driving an electrical power generator(s). The load compressor flow is regulated by a set of inlet guide vanes (IGV) located at the entry of the radial-to-axial intake. At full power, the IGVs are aligned radially (referred to as 0° setting), allowing maximum flow into the compressor. At fully closed position (about 85° setting), the IGV setting allows only about 5% to 7% leakage flow. Normally, when the IGVs are about half-closing (≈45°), a strong flow circulation Γ at the entry will be generated by the tangential flow components created by the IGVs. The circulation is convected towards the load compressor. As the flow area of the gaspath is reduced towards the load compressor, the initial circulation is stretched. This leads to an increase of vorticity intensity as a result of conservation of circulation. Normally, a vortex whistle will be generated when the stretched circulation is convected to approximately midway of the gaspath. There are few patents for vortex whistle suppression in radial-to-axial intakes. US patent 4436481 discloses an invention to suppress the vortex whistle by the installation of two tabs on two diagonally opposite IGV trailing edges. The idea is to disturb the strong initial circulation at the entry. US patent 4844695 discloses an invention of five fences at the mid gaspath on the hub surface. These fences will destroy the buildup of vorticity intensity at this critical location. This paper mainly reports the flow-noise characteristics associated with the fenced-intake (US patent 4844695), together with appropriate analytical review on vortex whistle in order to explain the experimental results.

2.0 Experiment

The test program was conducted during the development of a previous engine model which searching for feasible solutions of suppressing the intake vortex whistle. One of the experimental solutions was installing 5 fences in the gaspath. Test results were not published outside Pratt & Whitney Canada (PWC). The narrowband data is not available, and cannot be reproduced. However, sample of original narrowband data are provided to illustrate the noise spectra with and without vortex whistle tone.

Paper presented at the RTO AVT Symposium on "Habitability of Combat and Transport Vehicles: Noise, Vibration and Motion", held in Prague, Czech Republic, 4-7 October 2004, and published in RTO-MP-AVT-110.

2.1 Test Setup

The test was conducted at PWC's Intake & Exhaust Rig. In the test rig, a development intake was connected to a flow suction rig. The load compressor flow was simulated by the suction flow (Fig.1). All flow and noise measurements were made inside a test room. Tests were conducted with and without the fences (5) installed in the intake.

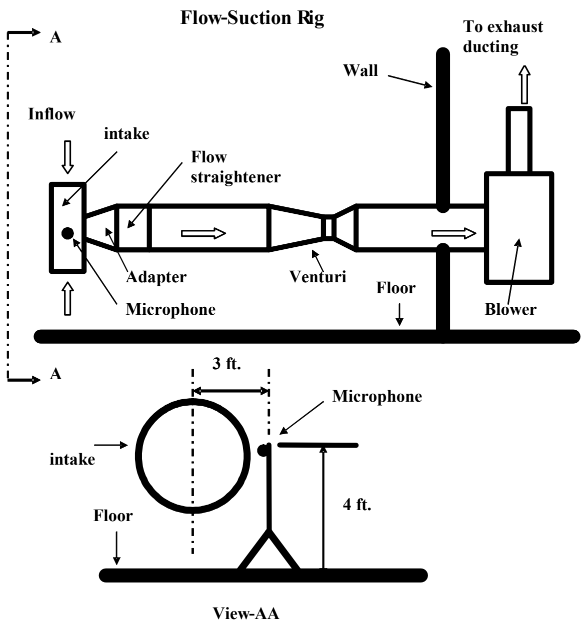

Fig.1 Test setup

Flow measurement

Flow measurement at the intake axial-exit face (i.e. load compressor inlet face) was achieved by a probe traversing unit. The unit consists of a specifically designed circumferential traversing gear, and a probe holder mounted on top of it. Three actuators were installed in the traversing system, allowing circumferential (60°), vertical (2.5”), and rotational (360°) movements of the probe (Fig.2).

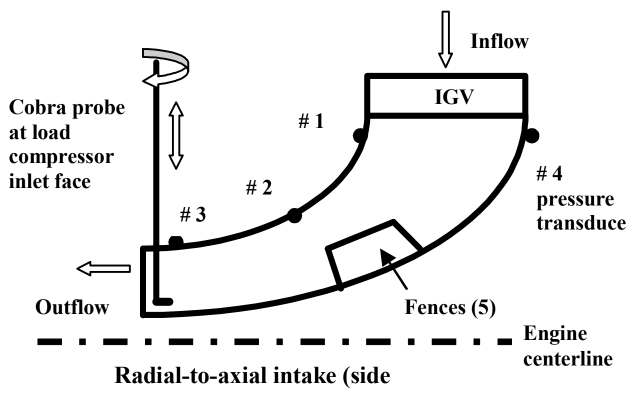

Fig.2 : Flow measurement setup :
flow traversing, and surface static pressure taps

Surface static pressure measurement

Three sets of static pressure taps (10 taps each) were installed at different locations relative to a fence location. Set #1 was evenly distributed along the centerline between two fences, from compressor inlet face to the IGV trailing edge. Sets #2 and #3 were installed circumferentially on the hub and shroud surfaces, covering a sector of 72° symmetrically with respect to a fence. Measurements were made using an automatic data recording (ADR) unit and a HP PC for data acquisition.

Four pressure transducers (Kistler) were installed along the intake gaspath. Three transducers were evenly distributed on the shroud surface, extending from compressor inlet face to IGV trailing edge. The fourth transducer was installed on the hub surface just downstream of the IGV trailing edge (Fig.2).

Noise measurement

A B&K microphone (0.5” dia., type 4134) with windshield was mounted on a tripod, which was positioned such that the microphone was 3’ from intake axis, 4’ from a side wall, 4’ above the floor, and 8’ below the ceiling. The microphone face was set parallel to the intake axis, pointing upward. The microphone and pressure transducer signals were recorded by a multi-channel magnetic tape recorded (Honeywell 101). A B&K high frequency resolution analyzer (type-2033) was used for visual display.

2.2 Test Procedures

A basic intake (without fences) flow characteristic was explored as a function of various IGV angle setting and massflow, in order to map out the occurrence of a vortex whistle. For a given IGV angle setting, the rig suction massflow was slowly increased to maximum until a vortex whistle was first detected. This was achieved by constantly monitoring the frequency spectrum display on the B&K-2033 frequency analyzer. A pure tone was usually first detected at low frequency starting at about 150Hz, depending on the IGV setting and massflow. After detecting the tone, the test was continued incrementally to higher massflow until maximum rig flow was reached. This test allows investigating the correlation of swirling flow frequency and vortex whistle frequency. During the noise survey, the frequency range was always scanned in order to check for the presence of any peculiar tones.

At selected IGV angle setting and massflow, all static pressures were recorded with an ADR unit. A 12-point traversing was conducted between the hub and the shroud gaspath surfaces at compressor inlet face. Only one circumferential position was required for the basic intake, but up to 5 circumferential locations symmetrically respect to a fence were conducted covering a sector of 72°.

3.0 Analytical Review

This section presents a review of analytical studies on vortex whistle, in order to explain the experimental flow-noise results.

Sound is emitted whenever a relative motion exists between two fluids or between a fluid and a surface. Physically, this is caused by the turbulent shear stresses at the interface. There are two classes of sound generation. One class is caused by the turbulence adjacent to solid surfaces, and the other one by velocity gradient between two fluid layers. Acoustic sources generated by the later type are often tonal, unstable, and susceptible to acoustic reinforcement. One essential ingredient of this type of unsteadiness is vorticity. In general, the flow induced noise requires the energy source in some form of flow unsteadiness. This unsteadiness does not need to be turbulent or random, as there are numerous cases of tonal sounds (whistles, cavity noise, singing propeller) that involve sinusoidal disturbances in the fluid.

3.1 Vorticity and Circulation Relation

Vortices, or eddies, are local rotating or spiraling fluid motions. They are usually associated with regions of flow transition that occurs at interfaces between fluids and solids in relative motions, or between parallel-mixing fluids of different velocity or density.

By definition, vorticity and circulation are determined by the following expressions respectively,

$$\mathbf{\Omega} = \frac{1}{2}\vec{\nabla} \times \mathbf{V} \qquad \text{(vorticity)} \tag{1}$$

$$\Gamma = \oint \mathbf{V} \bullet d\mathbf{L} \qquad \text{(circulation)} \tag{2}$$

and a *vortex line* is defined as a line drawn in fluid so that the tangent to it at any point has the direction of the axis of the vorticity at that point.

Let a continuous surface of arbitrary shape and orientation be superimposed on a given flow field containing vortices. Considering the surface to be subdivided into many small elements, it can be shown by Stokes' Theorem that

$$\Gamma = \oint \mathbf{V} \bullet d\mathbf{L} = 2\oiint \mathbf{\Omega} \bullet d\mathbf{S} \tag{3}$$

Equation (3) means that the total amount of circulation Γ around a closed circuit equals to the sum of the product of each vortex and its associated area.

3.2 Swirling Flow and Vortex Whistle Generation in Radial-to-Axial Intake

In turbulent flow, vorticity is responsible for regions of relatively intensive fluid activity and mixing. Sound is generated whenever a vortex line is stretched or accelerated relative to the acoustic medium [1].

In Fig.3, let the inflow contains an amount of circulation Γ_1 at station #1 as generated by the IGVs. The flow spirals towards the compressor inlet face at station #2 with circulation Γ_2. Due to symmetry, the vortex lines of the two circulations Γ_1 and Γ_2 coincide with the intake centre line.

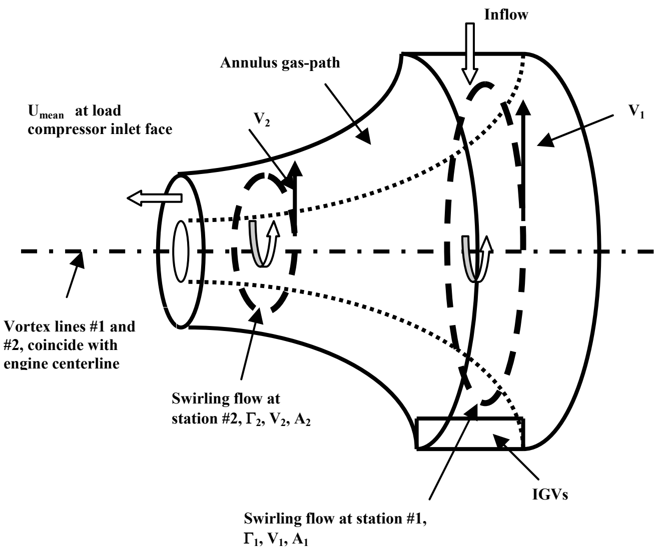

Fig.3 : Schematic swirling flow in a radial-to-axial intake

Neglecting losses, the total circulation is conserved. Therefore

$$\Gamma_1 = \Gamma_2 \tag{4}$$

where

$$\Gamma_1 = 2\pi r_1 V_1 \quad (5)$$

$$\Gamma_2 = 2\pi r_2 V_2 \quad (6)$$

and V_1, V_2 are the tangential flow components.

Since Γ_2 is associated with smaller flow area A_2 than that of Γ_1, the vorticity strength at station #2 is larger than that at station #1. This implies that the vortex line has been stretched. It is also accelerated by the increase of axial flow velocity as a result of reduced flow area. This explains how vortex sound is generated in a radial-to-axial intake with swirling inflow.

In this particular case, a pure tone (vortex whistle) is generated due to swirling flow as a periodic disturbance. This pure tone can be shown corresponding to the first tangential mode (m=1) of a spiral wave of $\cos(m\theta + kz - \omega t)$ [2]. In terms of acoustic annoyance and compressor efficiency, the vortex whistle is undesirable because of its intense tone and the associated higher aerodynamic loss.

In his work, Kurosaka [2] states that "vortex whistle is latent in swirling flow, emerging out of the selective amplifications of background disturbance''. In the radial-to-axial intake, the origin of the disturbance is the reduction of gaspath flow area, which accelerates and stretches the spiral flow. When the spiral flow reaches station #2 (somewhere in the gaspath, depending on the initially imposed flow circulation), the vorticity strength is increased. When the ratio of the peak tangential to mean axial velocity (V_{peak}/U_{mean}) exceeds certain value, the Reynolds shear stress is sufficient to generate sound (experimentally, a value of approximately √3 for this ratio was derived in the tested radial-to-axial intake).

Once the whistle is generated, its intense pressure field will modify the swirling flow from an originally almost free-vortex to a forced-vortex by acoustic streaming. This acoustic streaming is induced by organized periodic disturbance, rather than by random motions. It is shown that acoustic streaming induced by pure tone always produces incremental tangential velocity in the same direction as the swirling flow [2,3].

3.3 Total Temperature (Energy) Separation

3.3.1 Energy Equation

For a viscous, unsteady, compressible flow involving heat conduction and external body force, the energy equation [4] can be written as

$$\frac{D}{Dt}(H) = \frac{1}{\rho}\frac{\partial p}{\partial t} + \frac{1}{\rho}\frac{\partial}{\partial x_k}\left(u_j \tau_{jk} - q_k\right) + f_i u_i \quad (7)$$

where

$$\frac{D}{Dt} = \frac{\partial}{\partial t} + u_i \frac{\partial}{\partial x_i}$$

$h = c_p t$: enthalpy

$H = c_p T = h + \frac{1}{2} u_i u_i$: stagnation (total) enthalpy

$q_j = -k \frac{\partial T}{\partial x_j}$: heat flux per unit time

$$\tau_{ij} = \lambda \delta_{ij} \frac{\partial u_l}{\partial x_l} + \mu \left(\frac{\partial u_i}{\partial x_j} + \frac{\partial u_j}{\partial x_i} \right)$$: viscous stresses

f_i : external body force

u_i : velocity component

In the absence of appreciable heat conduction, viscous dissipation and external force, the energy equation is reduced to

$$\frac{D}{Dt}(H) = \frac{1}{\rho} \frac{\partial p}{\partial t} \tag{8}$$

This implies that any change in total temperature must associate with unsteady flow (the question is what kind of unsteadiness?), otherwise the total temperature is constant along any streamline.

On the other hand, if flow is steady, without heat conduction, and no external body force, the energy equation is reduced to

$$u_i \frac{\partial}{\partial x_i}(H) = \frac{1}{\rho} \frac{\partial}{\partial x_k}\left(u_j \tau_{jk}\right) \tag{9}$$

Equation (9) indicates that total energy change is entirely due to viscous stresses.

In most of aerodynamic problems the external body forces are negligible, and if a flow does not involve heat conduction, the total temperature change in that flow is attributed to both the unsteady and viscous effects. The relative importance of the two terms has remained a subject of controversy, and it probably depends on the type of flow considered. For inviscid flow, Liepmann & Roshko [4] indicated that the unsteady term is important in many nonstationary problems, such as the large temperature difference observed in the Hilsch tube. On the other hand, it is generally accepted that the energy separation is due to the combined effects of flow curvature, diffusion, dissipation, and not the unsteadiness. The argument is that most of the real vortex cores are turbulent. Therefore the turbulent effect must be included.

It is possible that there may exit many flows that satisfy the energy equation, resulting in total temperature separation. The swirling flow (an organized unsteady flow) is just one of the kind that can cause total temperature separation, depending on the flow conditions.

3.3.2 Energy Separation due to Turbulent Stresses

The Ranque-Hilsch effect, which separates the swirling fluid flow into an inner cold temperature and an outer hot temperature regions, can be considered due to turbulent energy transfer in general, and random migration of flow in the radial direction in particular.

In a steady, axisymmetric, turbulent swirling flow without external heat conduction and body forces, the total temperature change is attributed to the turbulent shear work, and the turbulent heat transfer by both temperature and pressure gradients. Although the terms for turbulent conduction due to temperature and pressure gradients are individually large, especially near the vortex center, they tend to cancel each other. Thus, the total temperature separation is mainly due to the turbulent shear work, and it is only possible in compressible flows [6].

In their work (Deissler & Perlmutter), the turbulent shear work done on a fluid is given by the term

$$W_s = \frac{1}{r} \frac{d}{dr}(rV\tau) \tag{10}$$

and the time-averaged Reynolds shear stress is determined by

$$\tau = -\rho\overline{uv} = \rho\varepsilon\left(\frac{dV}{dr} - \frac{V}{r}\right) \tag{11}$$

where V is the tangential velocity, u, v are the axial and tangential velocity fluctuations respectively, and $\rho\varepsilon$ is the eddy viscosity. In simple terms, positive shear work increases total temperature, whereas negative shear work decreases total temperature.

For a swirling flow in an annular duct, the tangential velocity distribution can be approximated by Rankine-vortex model (Fig.4), i.e. a viscous inner core region is surrounded by an effectively inviscid outer region. The velocity distributions are such that tangential velocity increases linearly with radius $(V \propto r)$ in the inner region, and decreases inversely proportional with radius $(V \propto 1/r)$ in the outer region.

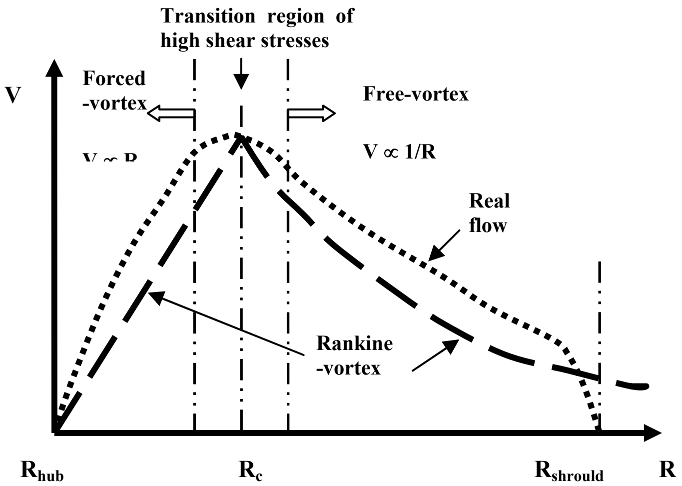

Fig.4 : Rankine-vortex model for tangential flow velocity

When examining the turbulent shear work (W_s) term, positive work is done on a fluid element in the outer free-vortex region, and negative work in the inner forced-vortex region. This causes the energy transfer (hence the total temperature separation). Therefore, energy separation depends on the radial distribution of tangential velocity profile.

In more precise terms, the shear work (W_s) can be decomposed into three components, consisting of dissipation (W_d), kinetic energy (KE), and potential energy (PE), i.e. $W_s = W_d + KE + PE$. Mathematically,

$$W_s = \frac{1}{r}\frac{d}{dr}(rV\tau) = \rho\varepsilon\left(\frac{dV}{dr} - \frac{V}{r}\right)^2 + \rho U\left(\frac{d\left(\frac{V}{2}\right)^2}{dr} + \frac{1}{\rho}\frac{dp}{dr}\right) \tag{12}$$

In the outer region, flow is effectively inviscid, the total energy (KE+PE) is constant, and hence its rate of change with respect to radial distance is zero. Therefore, the shear work is due to dissipation only.

In the inner region, dissipation becomes less important, because of wheel flow effect $(V \propto r)$, and hence KE and PE are dominant. In this region, both KE and PE are negative. Since static temperature across this region is approximately uniform, the total temperature will thus be lower near the centerline due to slower velocity. This is further enhanced by heat conduction towards the outer region by pressure gradient.

Deissler & Perlmutter [6] concluded that considerable amount of energy separation can be accounted for by considering only the steady-state effects, even though the unsteady-state effects are also contributors.

3.3.3 Energy Separation due to Unsteadiness

For an alternate explanation, Leipmann & Roshko indicated that the total temperature difference in a Hilsch tube is mainly due to the nonstationary term in the energy equation. Following their argument, Chu [3,5] concluded that acoustic streaming induced by organized unsteadiness (pure tone or vortex whistle), rather than random motion, is the mechanism of the Ranque-Hilsch effect.

In his work, Chu considered a flow in a vortex tube, consisting of a steady base flow and an unsteady disturbance with d.c. and a.c. components. The base flow, in turn, is assumed to be a helical form with constant axial and Rankine-vortex tangential velocity distributions.

$$\mathbf{u} = \mathbf{u}^*(r)\exp(i(m\theta + kz - \omega t)) \tag{13}$$

where $\mathbf{u}^*$ is the Fourier transform of $\mathbf{u}$ in m and k.

Near the surface, the local flow divides into two radial regions (Fig.4): a thin annular viscous region at the wall, corresponding to the steady and unsteady boundary layers, and an inviscid core outside of it [7]. Once the unsteady disturbances arise, the unsteady boundary layer emerges and becomes dominant over the steady one. This brings acoustic streaming into being out of the second order disturbance $\cos(2\omega t)$ in the viscous layer, due to the presence of high intensity pure tone.

The acoustic streaming induces an additional steady component in the same direction of the swirling flow. It occurs at the outer edge of the unsteady viscous layer, driving its steady counterpart in the surrounding inviscid region. This deforms the base Rankine-vortex into a forced-vortex, resulting in total temperature separation in the radial direction. The argument for the total temperature separation is based on the observations that once vortex whistle occurs, a forced-vortex tangential flow and a Ranque-Hilsch phenomenon occur coincidently. This is supported by the proof that, although the flow is turbulent, the forced-vortex generation is induced by the high intensity pure tone through acoustic streaming action, rather than by the turbulent random fluctuations

If radial entropy is constant, the total temperature separation is further enhanced by the larger static temperature gradient associated with a forced-vortex than that of a Rankine-vortex.

In Chu's conclusion, the Ranque-Hilsch effect is predominantly by acoustic streaming (i.e. due to organized unsteadiness) induced by the vortex whistle, and secondly by the total temperature gradient caused by viscous stresses.

4.0 Vortex Whistle Suppression

The fluid-body interaction is twofold. First, the body alters the sound pressure field radiated from turbulent sources by acting as a scattering or diffracting surface. Second, the body could alter the flow itself by creating additional flow disturbances in the form of vortices.

Flow over an obstructer consists of unsteadiness of free stream turbulence, boundary layer turbulence, trailing-edge flow separation and wake disturbances. These boundary disturbances generate a surface pressure field on the body. Sound pressure is therefore radiated. It should be noted that pressure associated with trailing-edge flow separation and wake could be tonal, depending on the regularity of the vortices. The net sound pressure from all sources depends on the amplitude and phase from each contributor. A sound signal can be viewed as a combination of a large number of superimposed sinusoidal acoustic sources. Mathematically, this is represented by a Fourier Series as

$$S(t) = \sum_{n=0}^{\infty} A_n \cos(2\pi f_n t - \phi_n) \tag{14}$$

where A_n, f_n, ϕ_n are the n^{th} signal's amplitude, frequency, and phase shift respectively.

Therefore, a combination of acoustic sources including *vortex whistle*, tip vortices, tones generated from trailing-edge flow separation, and wake, … etc, could result in reducing some tones.

In practice, tabs installed at the IGV trailing edges and fences in the mid-gaspath are examples of flow disturbers to suppress vortex whistle in a radial intake. The tabs generate turbulent zones. When these disturbing flows mixed with the main swirling flow, the swirl strength is reduced, preventing vorticity buildup. Thus vortex whistle is prevented. The fences destroy the swirling flow energy (particularly the tangential components) by predominantly a direct-impact action, and by secondarily a vortex-mixing action.

5.0 Experimental Results and Discussion

Flow measurement

Fig.5 shows the flow-noise characteristic of a development load compressor basic intake (without fences) as a function IGV setting and massflow. For the tested intake, vortex whistle first occurs only when IGV setting exceeds 45° (IGV setting convention: 0° is fully open, with IGVs set radially; 85° is fully closed, with IGVs set tangentially). This type of flow-noise characteristic is typical for radial-to-axial intake with inlet IGV at the entry. The vortex-whistle region is bounded between the intake flow capacity line (solid) and the vortex whistle starting line (dash). The actual engine operation can run into the vortex-whistle region when IGV setting exceeds 45°. Therefore, a solution of suppressing the vortex whistle is needed.

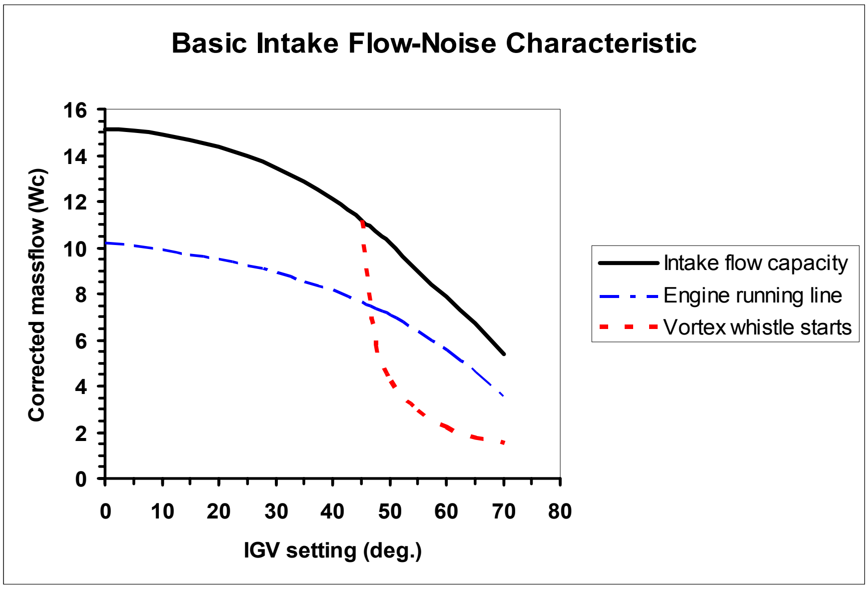

Fig.5 : Basic intake flow and vortex whistle characteristics

For the test intake, the first detected vortex whistle is at IGV angle of 45° and massflow rate of 11.3 lb/s. It was observed that the first tone disappears at reduced massflow. In general, when IGV angle exceeds 45°, there exist a critical massflow at which vortex whistle is first detected. Above this critical massflow, the vortex whistle intensity and its frequency increase with massflow. For massflow below this critical value, the vortex whistle disappears.

The critical massflow associated with each IGV setting was determined by observing the frequency shift of the pure tone on the B&K frequency analyzer display. The tone with heavy fluctuation was identified among other tones. It was observed that this particular pure tone (regarded as vortex whistle) was very sensitive to massflow changes.

Fig.6 shows the static pressure levels on the intake gaspath without vortex whistle. Results indicate that pressure transducer #4 on the hub surface just downstream of the IGV trailing edge appears to experience the highest static pressure drop.

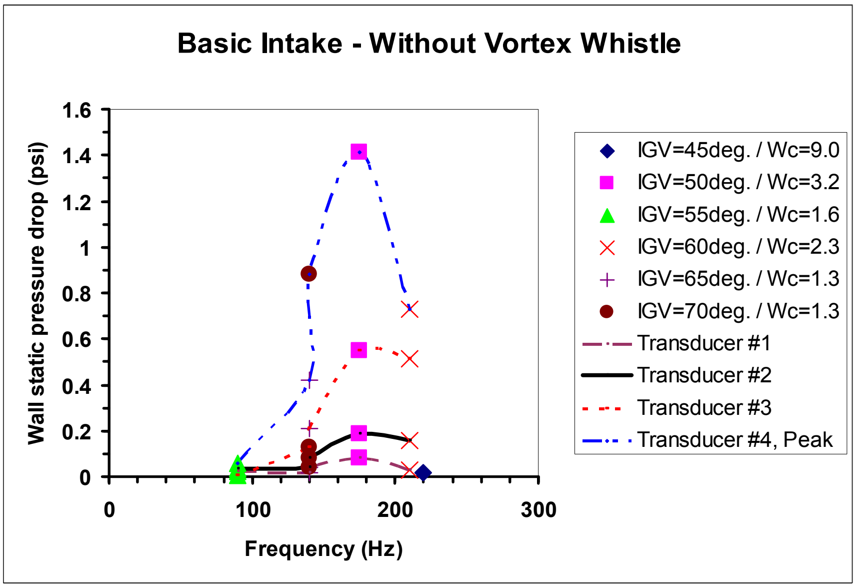

Fig.6 : Intake gaspath static pressure characteristics – Without vortex whistle

Fig.7 shows the static pressure levels on the intake gaspath with vortex whistle occurred. Results indicate that pressure transducer #2 on the mid-shroud surface appears to experience the highest static pressure drop. This suggests that the vortex whistle occurs at about mid-gaspath. It also indicates that pressure field pattern is peak at vortex whistle frequency of about 550Hz.

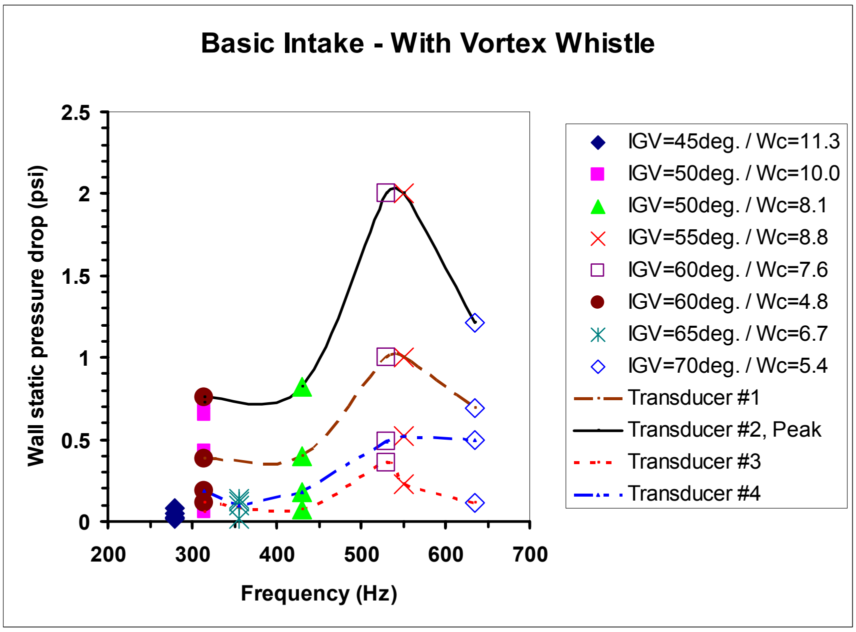

Fig.7 : Intake gaspath static pressure characteristics – With vortex whistle

Fig. 8 depicts the fence-wake development. Fig.9 depicts the vortex whistle free case. In preventing the vortex whistle generation, the periodic isolated fence-wake regions are generated. This induces periodic disturbance to the swirling flow. In Fig.10, when the wake regions start to merge, the induced periodic disturbance is lost. This could lead to re-generation of the vortex whistle.

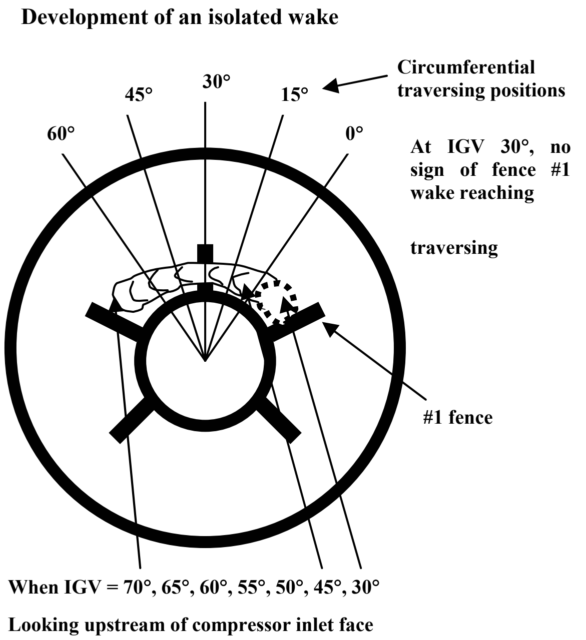

Fig.8 : Development of isolated fence-wake

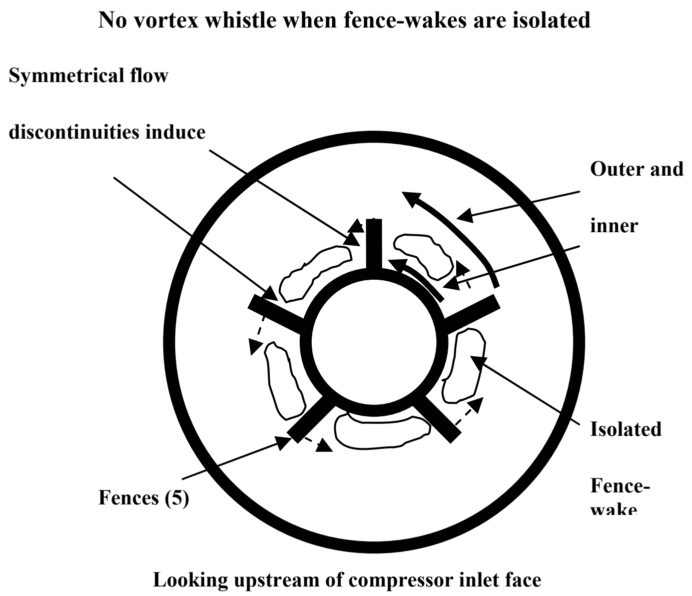

Fig.9 : Isolated fence-wakes induce periodic disturbances to the swirling flow

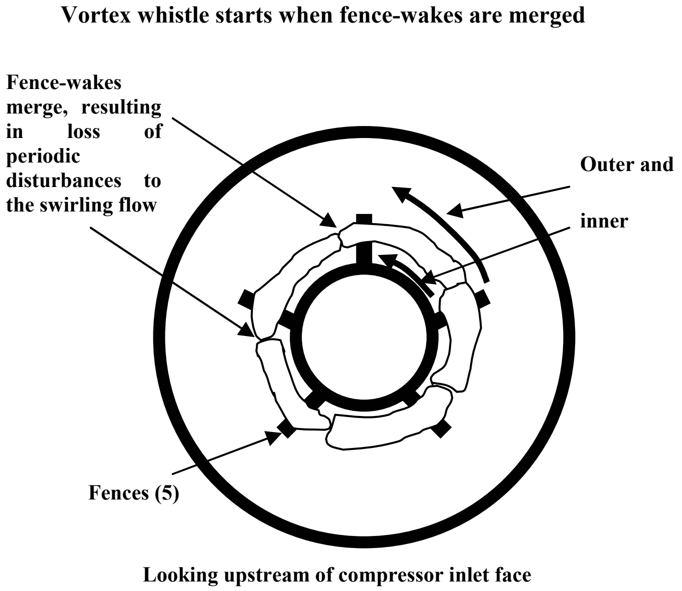

Fig.10 : Fence-wakes merge, resulting in loss of periodic disturbances

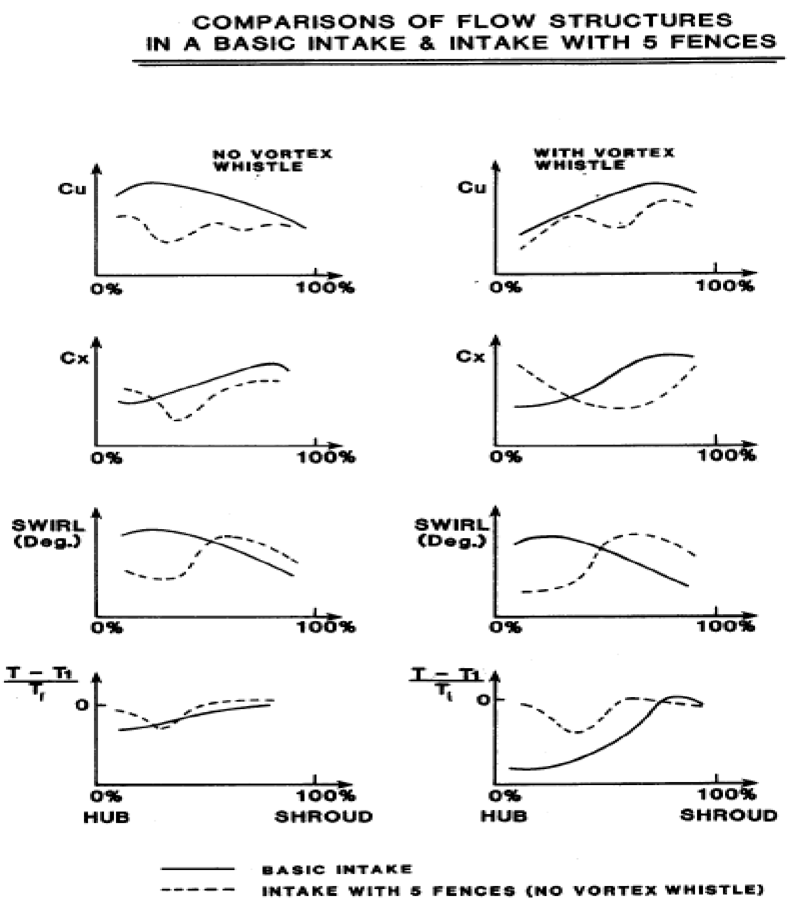

Fig 11 : Schematic flow comparisons with and without vortex whistle in both basic intake and fenced-intake

In summary, Fig.11 shows schematic comparisons of flow characteristics of a basic intake and intake installed with 5 fences. Measurements were made at load compressor face. In the figures, the solid line is for the basic intake, and the dash line for the intake with five fences installed.

Tangential flow velocity profile (Cu)
In the basic intake, the tangential flow velocity profile is deformed from a free-vortex to forced-vortex when vortex whistle occurs. However, for the fenced-intake, there is no significant and definite change in the tangential velocity profile. This is due to the fact that the fences disrupt the tangential velocity profile.

Axial flow velocity profile (Cx)
In the basic intake, the axial flow velocity profile is less disturbed when vortex whistle occurs, except with a slightly steeper slope variation from hub to shroud. However, for the fenced-intake, the axial velocity profile developed into a parabolic concave profile with minimum at about mid-span. This is due to the fence-wake blockage effect.

Flow swirl angle
Overall, there is no significant change of flow swirl orientation for both intakes either with or without vortex whistle. For the basic intake, the swirl profile appears to follow a free-vortex profile. For the fenced-intake, the swirl distribution is similar to a horizontal S-shape.

Total temperature profile
When vortex whistle is absent, there is no significant temperature separation. In the basic intake, without flow disruption, the temperature profile slightly decreases from shroud to hub. For the fenced-intake, a dip in temperature occurs at about 1/3 of the shroud-hub span. This corresponds to the fence-wake region. In the presence of vortex whistle, the total temperature distribution in the basic intake decreases drastically from shroud to hub, resulting in significant total temperature separation. In absolute term, a decrease of up to 20°F was observed during experiment. Whereas, there is practically not much change in the fenced-intake, except with a slightly larger temperature dip at about 1/3 of the shroud-hub span.

Noise measurement
In the following 1/3-octave spectrum plots, comparisons are presented between basic intake and fenced-intake.

IGV=45°
Figs. 12A and 12B show the noise spectrum comparison at 45° IGV setting at critical and reduced mass flows (11.3, 9.0 lb/s) respectively. At critical mass flow (Fig.12A), vortex whistle first detected at 200Hz band and this tone disappears at reduced massflow (Fig.12B). As expected, in both cases, the fences generate higher broadband noise at higher frequencies.

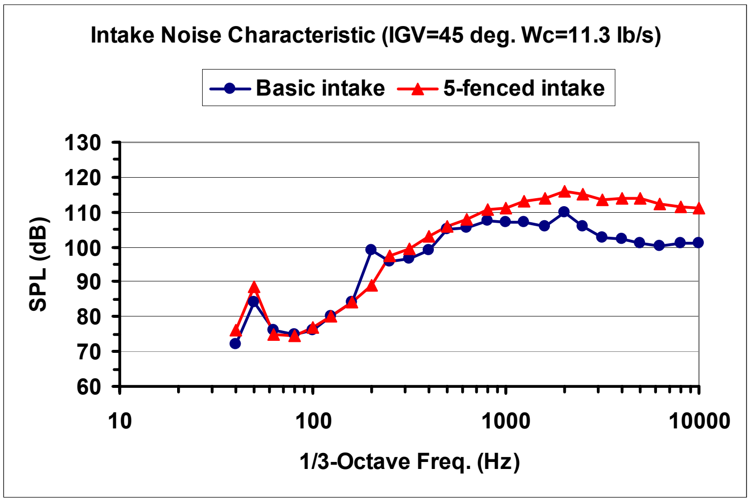

Fig.12A : Intake noise characteristic (IGV=45°, Wc=11.3 lb/s)

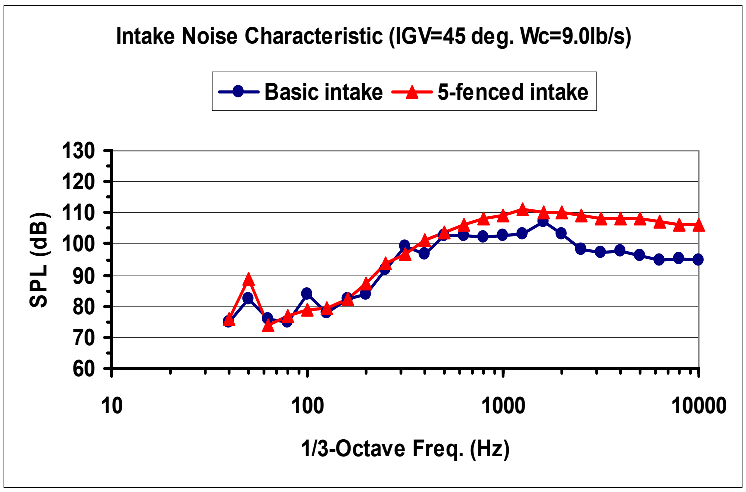

Fig.12B : Intake noise characteristic (IGV=45°, Wc=9.0 lb/s)

IGV=50°

Figs.13A, 13B and 13C show the noise spectrum comparison at 50° IGV settings with increasing massflows (6.0, 8.1,10.0 lb/s). The vortex whistle frequency increases with massflow, from 250Hz to 315Hz and 500Hz band. Basically, results indicate the fences are able to suppress the vortex whistle tone, but generate higher broadband noise at higher frequencies.

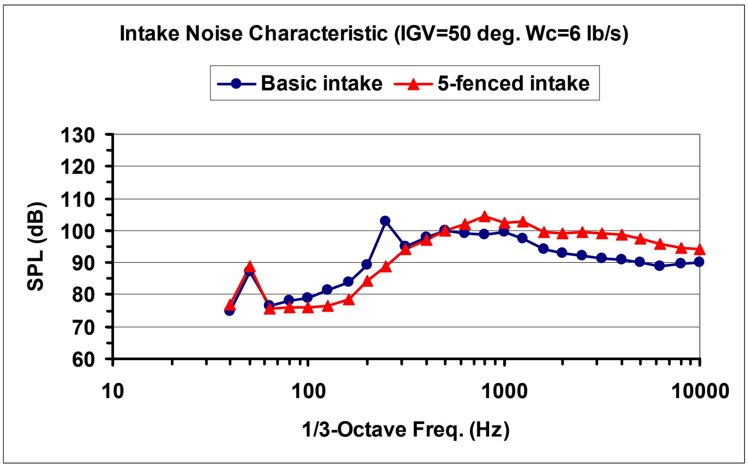

Fig.13A : Intake noise characteristic (IGV=50°, Wc=6.0 lb/s)

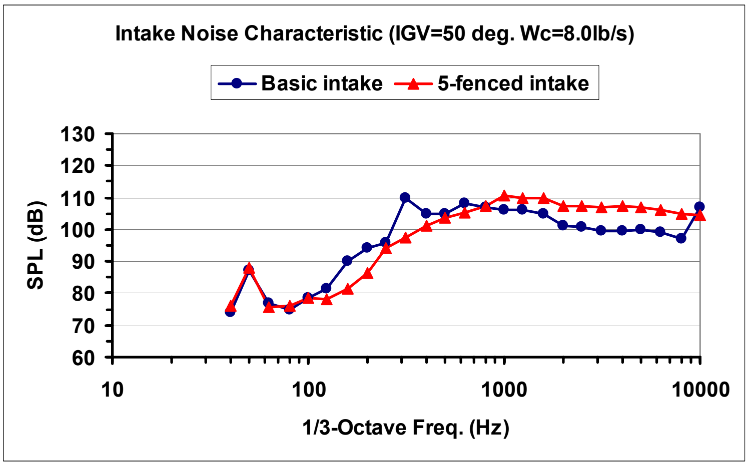

Fig.13B : Intake noise characteristic (IGV=50°, Wc=8.0 lb/s)

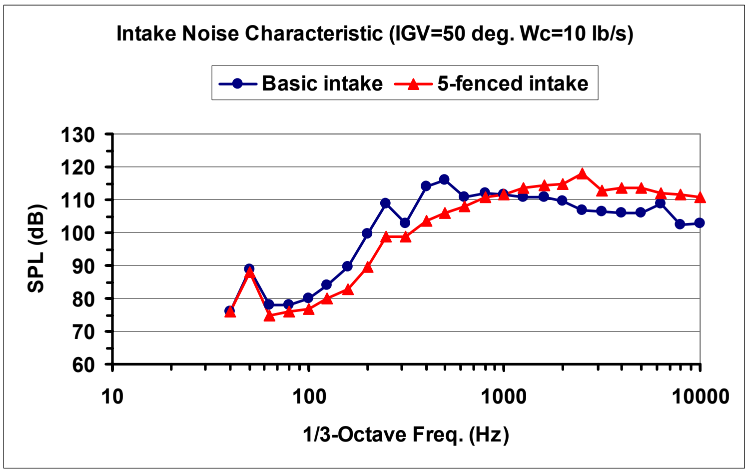

Fig.13C : Intake noise characteristic (IGV=50°, Wc=10.0 lb/s)

IGV=60°

Figs.14A and 14B show the noise spectrum comparison at 60° IGV settings with increasing massflows (4.8, 7.6 lb/s). The vortex whistle frequency increases with massflow, from 250Hz to 400Hz band. Results indicate the fences suppressing the vortex whistle, but generate higher broadband noise at higher frequencies.

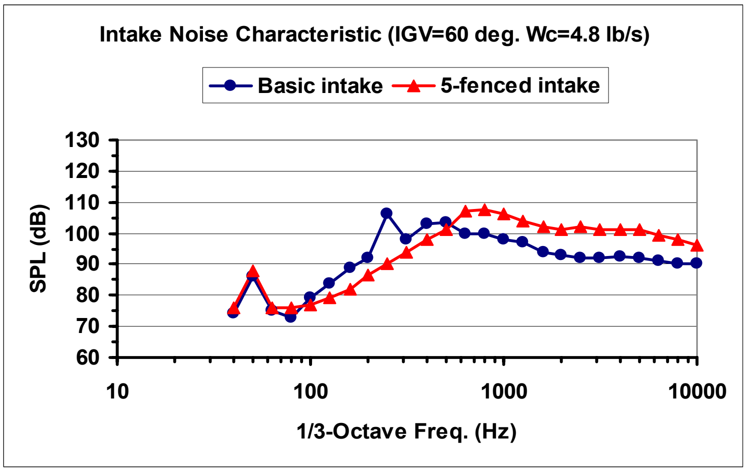

Fig.14A : Intake noise characteristic (IGV=60°, Wc=4.8 lb/s)

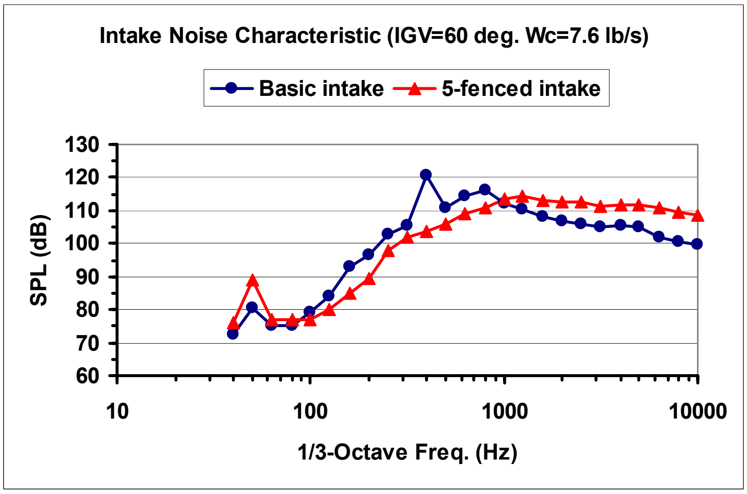

Fig.14B : Intake noise characteristic (IGV=60°, Wc=7.6 lb/s)

IGV=65°

Figs.15A, 15B and 15C show the noise spectrum comparison at 65° IGV settings with increasing massflows (3.5, 5.2, 6.7 lb/s). The vortex whistle frequency increases with massflow, from 250Hz, to 400Hz and 800Hz bands. Results indicate that the vortex whistle tone is suppressed by the fences, but with higher broadband noise at higher frequencies.

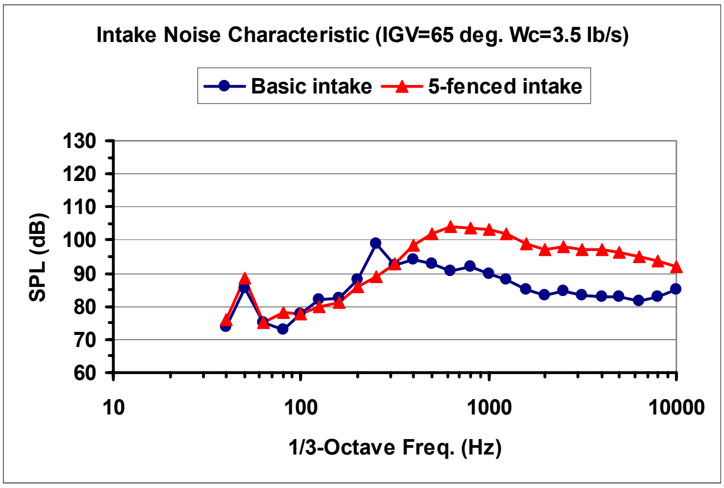

Fig.15A : Intake noise characteristic (IGV=65°, Wc=3.5 lb/s)

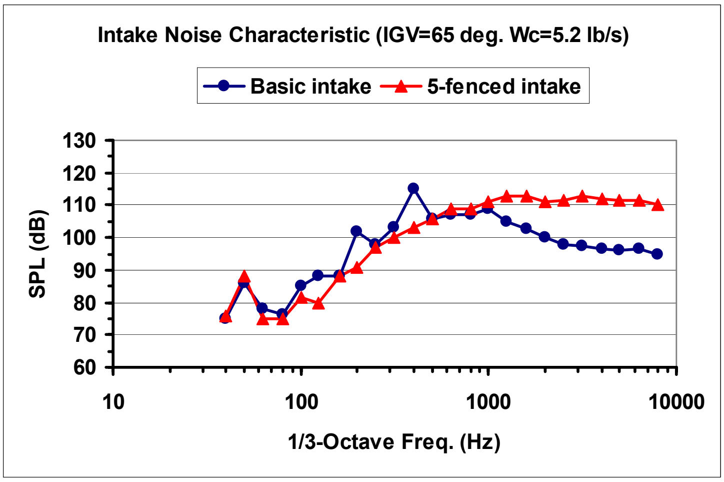

Fig.15B : Intake noise characteristic (IGV=65°, Wc=5.2 lb/s)

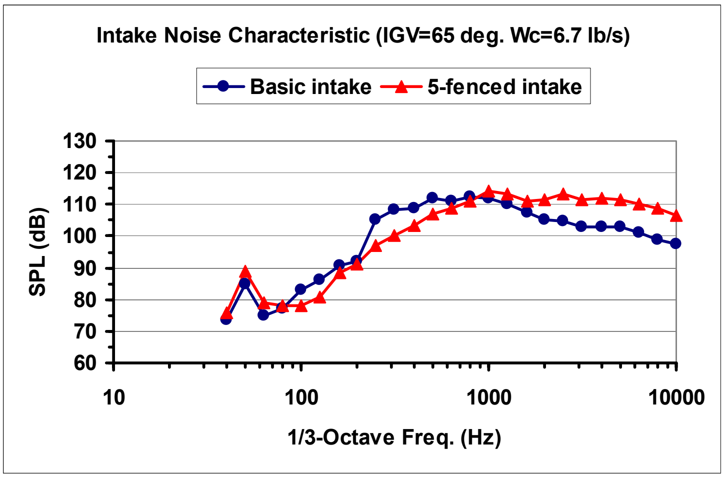

Fig.15C : Intake noise characteristic (IGV=65°, Wc=6.7 lb/s)

IGV=70°

Figs.16A and 16B show the noise spectrum comparison at 70° IGV settings with increasing massflows (2.5, 5.4 lb/s). The vortex whistle frequency increases with massflow, from 125Hz to 500Hz band. When IGV is at 70°, the swirling flow is generally very strong. At low massflow case (2.5 lb/s), results indicate that the vortex whistle tone is suppressed by the fences , but generates higher broadband noise at higher frequencies. At higher massflow (5.4 lb/s), the swirling flow is sufficiently strong such that vortex whistle remains in existence despite the presence of the fences.

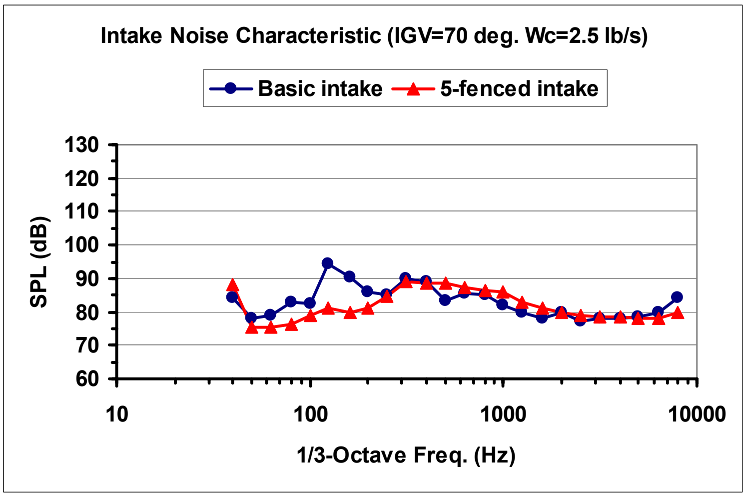

Fig.16A : Intake noise characteristic (IGV=70°, Wc=2.5 lb/s)

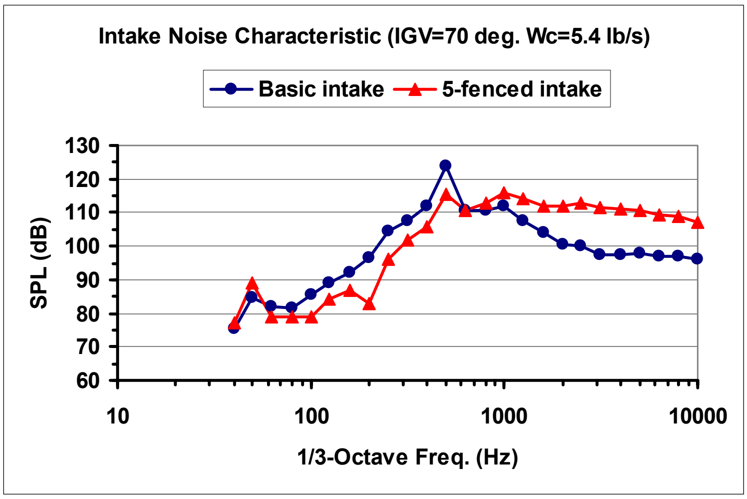

Fig.16B : Intake noise characteristic (IGV=70°, Wc=5.4 lb/s)

In summary, the fences are generally able to suppress the vortex whistle and reduce broadband noise at frequencies lower than the vortex whistle frequency. However, they generate higher broadband noise at frequencies beyond the vortex whistle frequency.

Correlation of vortex whistle fundamental frequency(f_o) with swirling flow frequency(f_s)
Considering conservation of circulation, the swirling flow frequency f_s is given by

$$f_s = \left(\frac{1}{2\pi}\right)^2 \frac{\Gamma}{R^2} \qquad (15)$$

Analytical review indicates [2,3] that the swirling frequency f_s is evaluated at the viscous core radius (i.e. $R = R_c > R_{hub}$) of a Rankine-vortex model. The circulation Γ can be estimated, knowing the inlet IGV throat area and its angle setting, and the amount of massflow.

As an approximation, the effect of R is also studied by assuming a free-vortex model with $R=R_{huh}$, evaluated on the hub surface. In Fig.17, the tangential flow velocity profile is modeled with a free-vortex profile, with the peak tangential velocity (V_{peak}) at the hub surface. Results indicate that the vortex whistle frequency f_o is about 2/3 of the swirling flow frequency f_s.

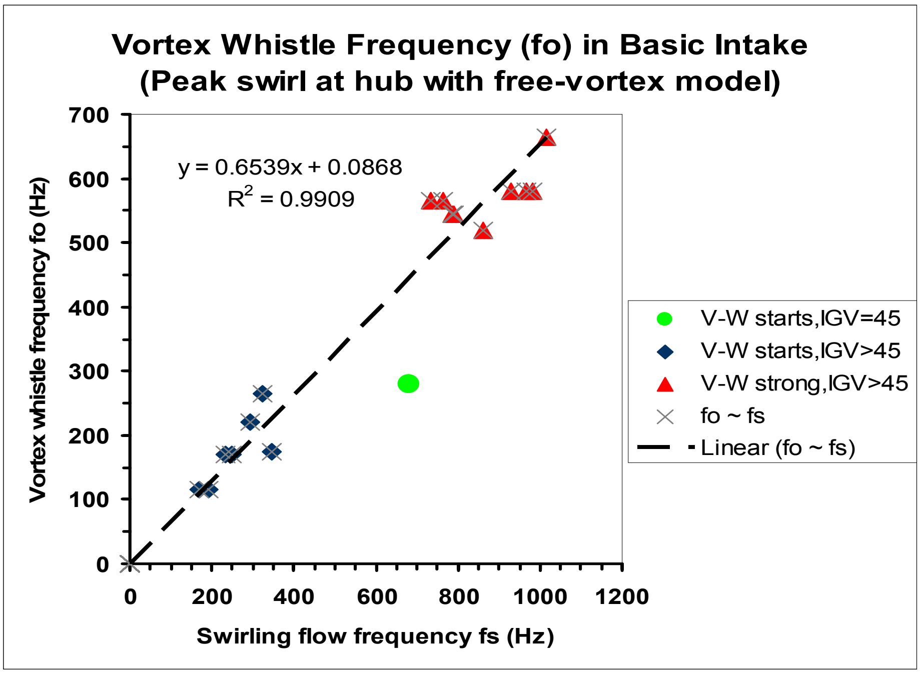

Fig.17 : Correlation of vortex whistle frequency with swirling flow frequency – Free-vortex model

In Fig.18, the tangential flow velocity profile is modeled with a Rankine-vortex distribution profile. Results indicate that vortex-whistle frequency f_o is equal to the swirling flow frequency f_s. This suggests that the tangential flow velocity profile follows that of a Rankine-vortex distribution. This is also in line with Kurosaka's theory [2].

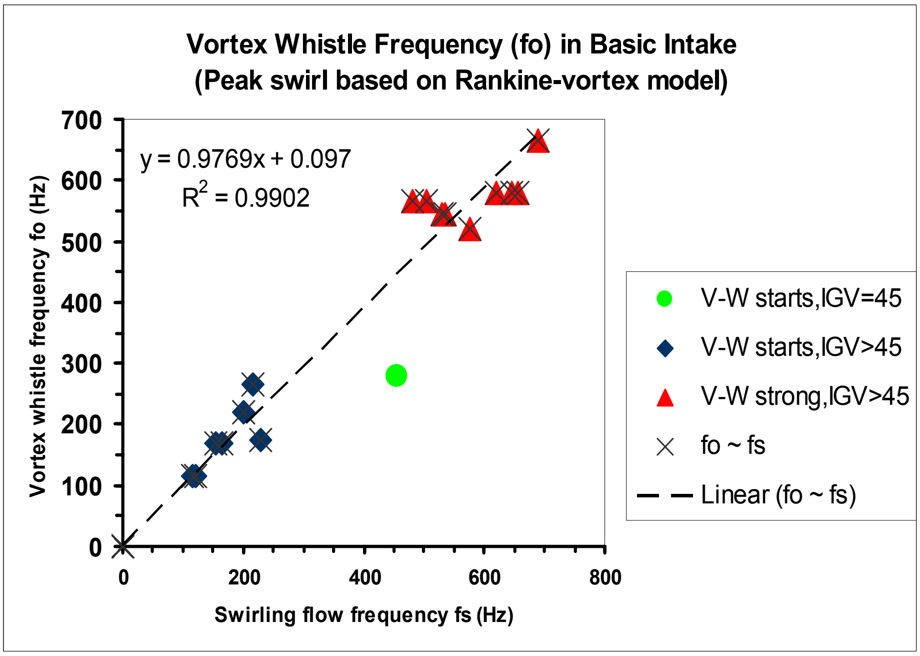

Fig.18 : Correlation of vortex whistle frequency with swirling flow frequency – Rankine-vortex model

Fig.19 shows correlation of $Sn_2 = V_{peak}/U_{mean}$ as a function of Reynold Number based on mean axial flow velocity (U_{mean}) at load compressor inlet face (i.e. $\mathrm{Re}_2 = U_{mean}(R_{shroud} - R_{hub})/\nu$). The peak tangential flow velocity is based on Rankine-vortex model. Results indicates that vortex whistle occurs only when V_{peak}/U_{mean} exceeding about √3.

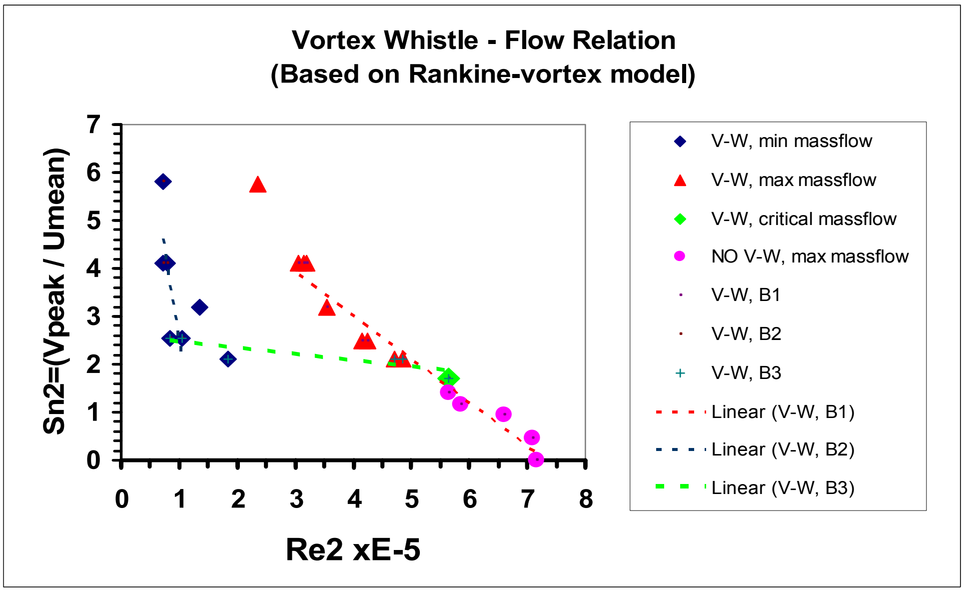

Fig.19 : Correlation for critical ratio of peak tangential to mean axial flow velocity. (B1, B2, B3 : are vortex whistle V-W boundaries #1, #2 and #3 respectively, where $\mathrm{Re}_2 = U_{mean}(R_{shroud} - R_{hub})/\nu$).

Other results

The following results could not be reproduced with better quality. Figs 20A and 20B show some typical narrowband spectra associated with and without vortex whistle. Results indicate that the vortex whistle occurs in the basic intake, but is successfully suppressed in a fenced-intake.

BASIC INTAKE | **INTAKE with 5 FENCES**

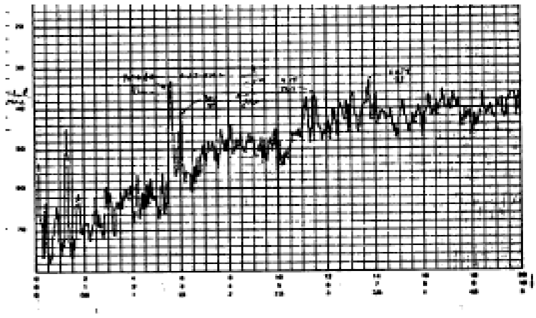

IGV=45° , Wc=11.3 lb/s

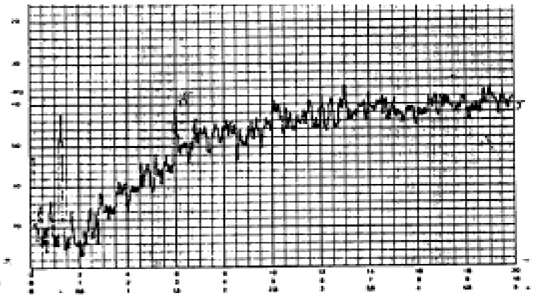

IGV=45° , Wc=10.9 lb/s

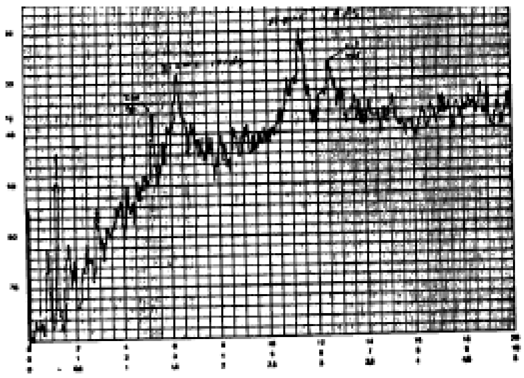

IGV=50° , Wc=10.0 lb/s

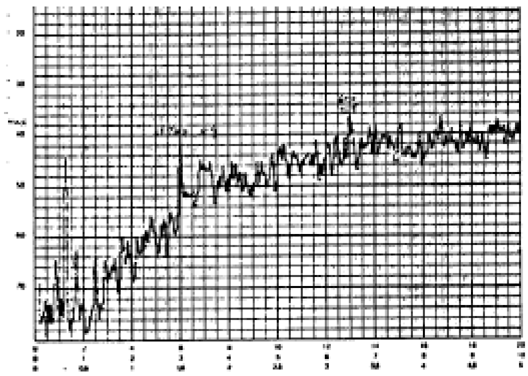

IGV=50° , Wc=9.9 lb/s

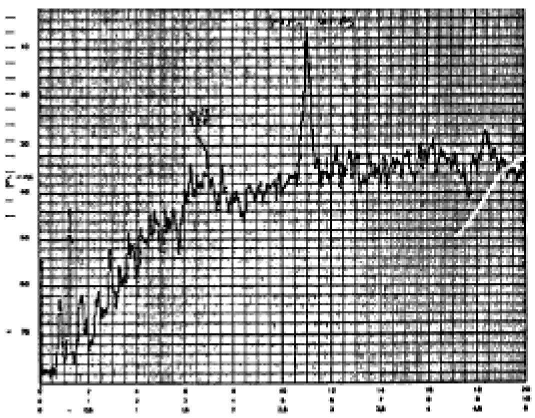

IGV=55° , Wc=8.8 lb/s

Fig.20A : Narrowband noise spectra with and without vortex whistle at IGV of 45°, 50°, 55°
(The spiky pure tone is the vortex whistle tone)

BASIC INTAKE **INTAKE with 5 FENCES**

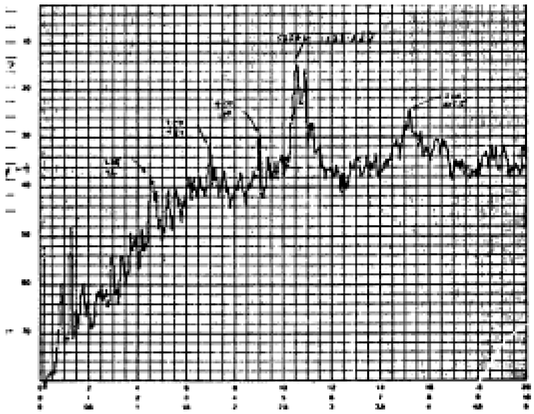

IGV=60° , Wc=7.6 lb/s

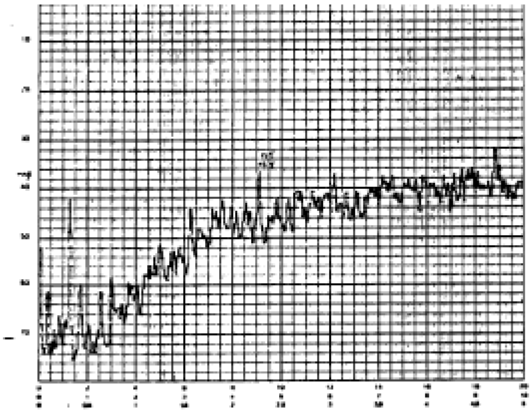

IGV=60° , Wc=7.5 lb/s

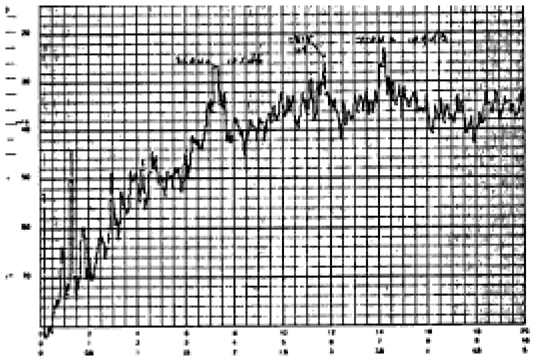

IGV=65° , Wc=6.7 lb/s

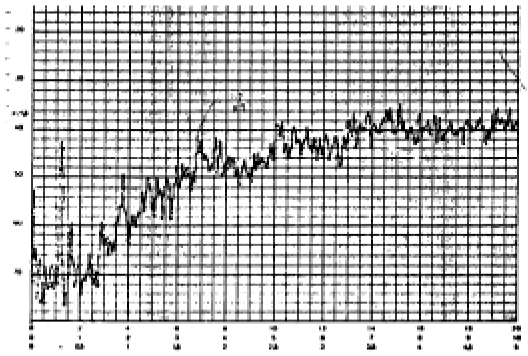

IGV=65° , Wc=6.1 lb/s

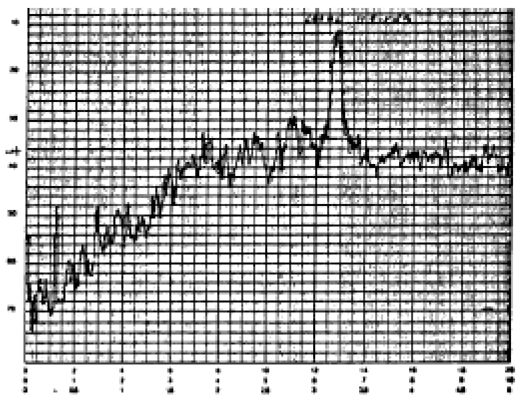

IGV=70° , Wc=5.4 lb/s

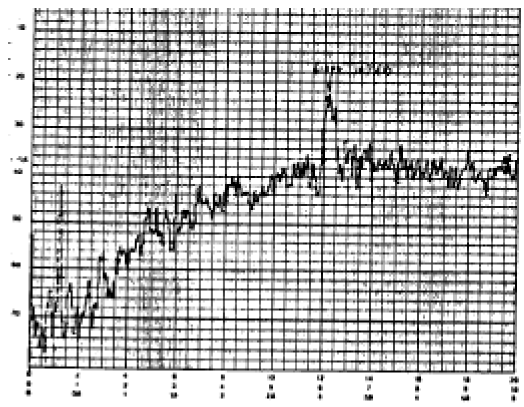

IGV=70° , Wc=4.5 lb/s

Fig.20B : Narrowband noise spectra with and without vortex whistle at IGV of 60°, 65°, 70°
(The spiky pure tone is the vortex whistle tone)

6. Conclusion

A radial-to-axial intake with sufficient circulation imposed at the radial entry will generate whistle vortex somewhere in the gaspath. Experimentally, a fenced-intake was found capable to suppress vortex whistle, but generating higher broadband noise at frequencies above the vortex whistle frequency. Experimental results demonstrate that the vortex whistle fundamental frequency (f_o) is equal to the swirling flow frequency (f_s) evaluated at the viscous core of a Rankine-vortex model for the tangential flow velocity. Results also indicate that vortex whistle occurs only when V_{peak}/U_{mean} exceeds about √3.

In simple terms, any device generating sufficient disturbances to the swirling flow in preventing buildup of vorticity strength will be able to suppress the vortex whistle. In practice, any object inserted into the swirling flow field can create disturbances, consisting of a direct-impact action, and a vortex-mixing action. The relative importance of each action depends on the flow-disturber in the intake assembly. The choice of disturber-intake assembly should give minimum disturbance to the vortex flow field, while achieving vortex whistle suppression.

7. References

[1] "Theory of vortex sound'', A. Powell, J. Acoustical Soc. Amer., vol. 33, No.1, 1964, pp. 177-195.

[2] "Acoustic streaming in swirling flow and the Ranque-Hilsch (vortex-tube) effect'', M. Kurosaka, J. Fluid Mech. Vol. 124, 1982, pp.139-172.

[3] "Acoustic Streaming as a Mechanism of the Ranque-Hilsch Effect'', Joseph Quang Chu, PhD discertation, December 1982, The university of Tennessee.

[4] "Elements of Gasdynamics'', H.W. Leipmann , A. Roshko, John Wiley & Sons Inc., 1957, pp. 190, 337

[5] "An interplay between acoustic waves and steady vertical flow'', M. Kurosaka, J.R. Goodman, J.Q. Chu, H. Kuroda, AIAA 8th Aeroacoustics Conference, 11-13/April/1983.

[6] "Analysis of the flow and energy separation in a turbulent vortex'', R.G. Deissler and M. Perlmutter, Int. J. Heat Mass Transfer, vol.1, 1960, pp.179-191.

[7] "Turbulent swirling pipe flow'', Chiaki Huroda , Kohei, Ogawa, Chapter 20, Encylopedia of Fluid Mechanics vol. 1, 1986, Gulf Publishing Co.

Detailed Analysis or Short Description of the AVT-110 contributions and Question/Reply

The Questions/Answers listed in the next paragraphs (table) are limited to the written discussion forms received by the Technical Evaluator. The answers were normally given by the first mentioned author-speaker.

P22 M-C. Tse 'Vortex Whistle in Radial Intake' (P&W Canada, CA)

In the category of the 'Technical Engineering' , this excellent analytical study of the flow circulation generated by the radial-to-axial intake of the compressor as used in an auxiliary power unit (APU) lead the author to propose the introduction of fences around the intake to suppress the vortex whistle: the experimental results were largely explained by his analytical model.

Discussor's name: R. Peterson
Q. Does the introduction of the fences in the turbine produce a loss in power or efficiency?
R. Yes, any solid deject (disturber, such as fences) will introduce aerodynamic losses, which is in fact not favorable to the compressor system. However, this is one of the most feasible solution for implementation, considering other constraints and other solutions.